Progress in Organic Coatings 77 (2014) 1073–1078

Contents lists available at ScienceDirect

Progress in Organic Coatings

journal homepage: www.elsevier.com/locate/porgcoat

Short communication

Effect of 3-Aminopropyltriethoxysilane on polycarbonate based waterborne polyurethane transparent coatings

Haifeng Zhou[a], Hua Wang[a], Xingyou Tian[a,*], Kang Zheng[a], Qingtang Cheng[b]

[a] Key Laboratory of Materials Physics, Institute of Solid State Physics, Chinese Academy of Sciences, Hefei 230031, China
[b] Jiangsu Hehai Nanometer Science and Technology Co., Ltd., Taixing 225401, China

ARTICLE INFO

Article history:
Received 13 August 2013
Received in revised form 15 January 2014
Accepted 13 March 2014
Available online 9 April 2014

Keywords:
Polyurethane
Transparent coating
3-Aminopropyltriethoxysilane

ABSTRACT

A series of waterborne polyurethane (WPU) dispersions modified with different contents of 3-aminopropyltriethoxysilane (APTES) were synthesized based on poly(1,6-hexyl 1,2-ethylcarbonate) diol (PHEC) and isophorone diisocyanate (IPDI), and the films were obtained by casting the dispersions on Teflon molds. Effects of APTES content on the particle size and viscosity of the dispersions were studied. The structure and properties of the resulting films were investigated by Fourier transform infrared spectroscopy, wide angle X-ray diffraction measurement, dynamic mechanical analysis, thermogravimetric analysis and mechanical testing. The experimental results showed that the incorporation of APTES played an important role in the enhancement of the water and toluene resistance and mechanical properties of the SPU films. Young's moduli and ultimate tensile strengths were improved from 8.0 to 451 MPa and 6.5–19 MPa respectively as the APTES content increased from 1 wt.% to 20 wt.%. The ability of scratch resistance was enhanced, when the content of APTES increased to 20 wt.%, the 3H pencil could not mar the surface. Moreover, the transmittance spectra indicated that the coatings showed high transparence.

1. Introduction

Polyurethanes (PUs), most versatile classes of polymers, are used extensively in applications from foams and elastomers to adhesives and coatings [1–7]. The wide applicability of PU is due to the flexibility in selection of monomeric materials from a great variety of diisocyanates, macrodiols and chain extenders, as well as the ability to form different types of molecular architectures specifically tailed for each application. However, the conventional PU products usually contain a large number of organic solvents and sometimes even free isocyanate monomers which are harmful to the environment and human health. Therefore, they have been gradually replaced by the (WPU) in the past decades [8–14].

WPU are binary colloidal systems in which the particles of PU are dispersed in a continuous water phase. They have been used in various fields including as coatings, printings and adhesives because of environmental advantages. However, the thermal stability, water resistance, and mechanical properties of the WPU are needed to be improved compared with the organic solvent based PU. Great efforts have been devoted to speeding up the developments of WPU. For example, organic–inorganic nanocomposites have been developed to combine the desirable properties of WPU with inorganic fillers. Various types of filler, such as clay, cellulose, silica and starch nanocrystals were used, and the tests demonstrated significant improvement of the performances such as mechanical properties, thermal stability and others [15–18]. Moreover, various WPU/acrylic hybrid dispersions were carried out to offer synergetic proprieties through different routes, such as seeded emulsion polymerization, miniemulsion polymerization, interpenetrating polymer networks (IPN) and so on [19,20]. Additionally, some other materials, e.g., epoxy resin, polysiloxane and alkoxysilane have also been used to incorporate into polyurethane backbone to improve WPU proprieties [21,22]. Among the above-mentioned methods, modification of WPU with APTES is an important and effective way to prepare high performance materials [13,23]. The introduction of APTES into polyurethane backbone can be carried out easily through the terminal amine group of APTES reacting with the functional group of diisocyanate. Silanized polyurethane contain the condensable terminal groups and the sol–gel reactions take place during the phase inversion process which involve the hydrolysis and polycondensation reactions of silicon alkoxides and give rise to a stable siloxane crosslinked WPU.

Polycarbonate (PC) based polyurethanes have been studied and exploited especially for high transparent coatings due to the superior proprieties of PC such as great toughness, flexibility, durability, hydrolysis resistance, oil resistance and high transparence [24,25].

* Corresponding author. Tel.: +86 55165592752; fax: +86 55165591434.
E-mail address: xytian@issp.ac.cn (X. Tian).

http://dx.doi.org/10.1016/j.porgcoat.2014.03.006
0300-9440/

The purpose of this study is to prepare a series of PC based WPU dispersions with different contents of APTES and investigate the effects of APTES on the viscosity and particle size of the dispersions, and the thermal properties, mechanical properties, optical properties of the films.

2. Experimental

2.1. Materials

Isophorone diisocyanate (IPDI), 2-dimethylol propionic acid (DMPA), poly(1,6-hexyl 1,2-ethyl carbonate) diol (PHEC) (Mw = 2000), were supplied by An Li Artificial Leather Co., Ltd., Hefei, China. Sodium hydroxide and hydrochloric acid, dibutylamine, dibutyltin dilaurate (DBTDL), ethylene glycol (EG), triethylamine (TEA) were purchased from Su Yi Chemical Reagent Co., Ltd., Shanghai, China. Acetone (Ac), toluene, 3-aminopropyltriethoxysilane (APTES) were purchased from Qiang Shen Chemical Reagent Co., Ltd., Nanjing, China. The raw materials were used as received, except for the PHEC which were dried in vacuo at 100 °C for 2 h.

2.2. Preparation of SPU

The silanized WPU (SPU) was prepared by the acetone process. The PHEC (90 g), IPDI (40 g), and DMPA (4.4 g) were added to a four-necked flask equipped with a mechanical stirrer, nitrogen inlet, condenser, and thermometer. The reaction mixture was stirred and carried out at 80 °C for 1 h under a dry nitrogen atmosphere. Upon reaching the theoretical NCO value (6.4 wt% NCO) which was determined by a dibutylamine back titration method, EG (5.3 g) and DBTDL were added. Stirring was continued for 30 min at 60 °C and then AC was added to reduce the viscosity of the system. After an additional 3 h of reaction, APTES (1.4 g) was added and allowed to react with the remaining free isocyanate groups at 50 °C for 1 h, then the reactants were cooled to room temperature and neutralized by the addition of TEA (3.3 g) for 30 min to neutralize all the carboxylic acid groups at 40 °C. At the end, water was added to accomplish the dispersing at high speed. Finally, Ac was removed using distillation equipment. The solid content of the resulting dispersion was comprised between 30%. The dispersions were poured into Teflon molds to dry at ambient temperature for 7 days to obtain transparent films. The compositions of other samples are given in Table 1.

2.3. Characterization

Fourier transform infrared (FTIR) spectroscopy was performed on a spectrometer (Nexus, Nicolet) using the attenuated total reflectance (ATR) technique. Data were collected at 4 cm^{-1} resolution co-adding 32 scans per spectrum. Wide angle X-ray diffraction measurement was carried out with a Philips X'pert-PRO using Cu-Ka radiation. The diffraction angle 2θ ranged from 10 to 90°. The particle size and viscosity of the dispersions were measured with a Malvern Zetasizer and a Brookfield Viscometer (NDJ-5S) at 25 °C. The dispersions were kept in sealed bottles at room temperature to examine the storage stability. Dynamic mechanical tests were performed using a dynamic mechanical thermal analyzer (DMTA) (Pyris Diamond DMA, Perkin-Elmer) at 1 Hz, 5 °C/min from −80 °C to 200 °C. The tensile properties of the films were measured at 25 °C with a universal testing machine (CMT, SANS) at a crosshead speed of 300 mm/min. The reported values are averages obtained from five specimens. Thermogravimeter (Pyris 1 TGA) was used to measure the weight loss of the SPU films under N_2 atmosphere. The samples were heated from 100 °C to 700 °C at a heating rate of 10 °C/min. Pencil hardness was carried out by a pencil hardness tester (Pushen) according to the State Standard Testing Method (GB/T 6739-2006, equivalent of ISO 15184). The SPU were coated on glass and the final thickness of the films was about 100 μm. The transmittance of the glass with the SPU coatings were measured by UV360 (Shimadzu) UV–VIS–NIR spectrophotometer. The transition mode was used and the wavenumber range was set from 400 to 780 nm. The refractive index of SPU-0 was measured by Automatic Digital Refractometer (RA-620). The surface morphology of the SPU samples was analyzed by field emission scanning electron microscopy (FESEM, Sirion 200 FEI). Samples were adhered to aluminum sample holders and sputter coated with Au layer. TEM of the diluted SPU dispersions were obtained with a transmission electron microscope (JEM-2010). The swelling ratios of the SPU films were determined as follows. Samples of 1 g were cut from the SPU films, weighed, and then immersed in water or toluene for 24 h at room temperature. After the residual solvent was wiped from the film surface with filter paper, the weight of the swollen film was measured immediately. The swelling ratio was expressed as the weight percentage of solvent in the swollen film:

$$\text{swelling ratio} = \frac{W_s}{W_d}$$

where W_s is the weight of the swollen film and W_d is the weight of the dry film.

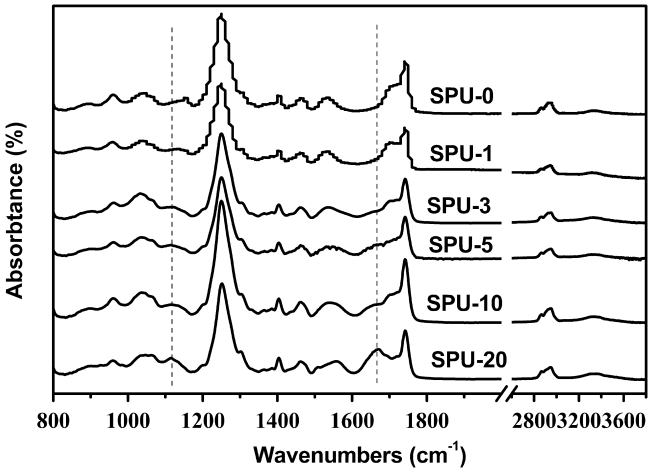

Fig. 1. IR spectra of the SPU.

3. Results and discussion

3.1. FT-IR

FT-IR spectroscopic measurements were performed to identify SPU with different APTES contents. The samples were analyzed in the form of films. In Fig. 1, the FTIR spectra of the SPU are presented with absorption peaks assigned according to the literature [26]. For SPU containing PHEC, a pronounced peak at 1250 cm^{-1} characteristic of the carbonate group (—O—C(=O)—O) are significant. The absorption bands around 3343 cm^{-1} (N—H stretching), strong absorptions at 1740 cm^{-1} (free C=O stretching of urethane and carbonate groups), 2940 and 2861 cm^{-1} (the CH_2 anti-symmetry and symmetry stretching vibrations), 1113 cm^{-1} (C—O—C stretching vibration of PC and Si—O—Si asymmetric stretching vibration) confirm the formation of the urethane linkage. The band of 1670 cm^{-1} assigned to the carbonyl stretching vibrations of urea groups generated as a consequence of the reaction between isocyanate and APTES amine groups. The insertion of APTES into the polymer chains can be confirmed by the broadening of the band at 1670 cm^{-1} and 1113 cm^{-1}.

Table 1
Formulations to SPU, swelling properties and TGA for SPU films.

Sample	APTES (wt.%)	IPDI (g)	PCD (g)	DMPA (g)	EG (g)	TEA (g)	APTES (g)	S_W (%)[a]	S_X (%)[b]	T_{10}) (°C)[c]	T_{50} (°C)[d]
SPU-0	0	40	90	4.4	5.3	3.3	0	22	Soluble	290	330
SPU-1	1	40	90	4.4	5.1	3.3	1.4	16	230	294	338
SPU-3	3	40	90	4.4	4.7	3.3	4.2	14	162	291	339
SPU-5	5	40	90	4.4	4.3	3.3	7.0	5	139	296	343
SPU-10	10	40	90	4.4	3.4	3.3	14	1.3	128	292	345
SPU-20	20	40	90	4.4	1.4	3.3	28	0.5	105	302	356

[a] Swelling of SPU films in water.
[b] Swelling of SPU films in toulene.
[c] 10% weight loss temperature (°C).
[d] 50% weight loss temperature (°C).

Further analysis of the FTIR spectra of the SPU could be used to investigate the absorption peaks of the urethane and urea groups and provide information on the hydrogen bond formation. The absorption bands around 3343 cm^{-1} corresponded to the hydrogen-bonded N—H stretching vibration are pronounced. The band at 3400–3500 cm^{-1} assigned to non-hydrogen-bonded N—H stretching is not found in the spectra indicating that the amide groups in the SPU films are all involved in hydrogen bonding. Moreover, the urea (C=O) peak at 1630 cm^{-1} in the hard segment are not observed and the intensity of the urethane (C=O)1700 cm^{-1} decreases with increasing APTES, both of these two bands are corresponded to the formation of ordered hydrogen bonds. In addition, the disordered hydrogen bonded C=O peak of urea (1660–1670 cm^{-1}) is present in the spectra and its intensity increases with increasing APTES. Thus, it is concluded that the APTES leads to an increasing urea contents in the resulting materials and stronger phase mixing on the interface between hard and soft segments and therefore more amorphous hard segment phase. The spectroscopy findings correlate well with changes in morphology and thermal and mechanical properties, as discussed below.

3.2. The effect of APTES content on the SPU dispersions

Usually, PU polymers are not soluble in water. WPU can be prepared by incorporating hydrophilic groups in the polymer backbone or by adding a surfactant. In this work we used DMPA as the internal emulsifier which reacted with TEA and formed ammonium carboxylate anions [$COO^-HN^+(C_2H_5)_3$] to stabilize the particles. The average particle size and viscosity are important and affect the colloidal stability of dispersions. Fig. 2 shows the average particle size and viscosity as a function of APTES concentration. It is found that the average particle size and viscosity changed slightly as APTES content increased from 0 wt.% to 10 wt.%, however, as it increased to 20 wt.%, the particle size increased to 110 nm and the viscosity decreased to 55 mpa s. That the larger particle sizes and lower viscosity are obtained may be due to (1) the crosslinking density increases as APTES increasing because of the condensation of alkoxysilane groups taking place in the process of dispersion and the phase inversion become difficult especially for high APTES content (2) the urea groups are less hydrophilic than urethane groups and more urea groups are formed as demonstrated in Section 3.1 (3) the Si—O—Si unit is hydrophobic [13]. Moreover all the dispersions are stable than 6 months.

3.3. X-ray diffraction

X-ray diffraction analyses of the SPU with different APTES contents are shown in Fig. 3. Each SPU exhibits a broad diffraction halo at $2\theta = 20°$, which is the same as that of the pure WPU. These diffraction halos indicate the formation of the amorphous phase of SPU and some aggregated hard segment domain resulted from the phase separation [27]. As the APTES content increases, such a diffraction peak becomes weaker and broader. Two factors may be responsible for this observation. First, the strong phase mixing on the interface between hard and soft segments disturbs the ordered arrangement of polymer chains. This fact confirms the results of the FTIR spectra analysis. Second, the average chain length is shorter as more APTES added, which is not favorable to crystallization.

3.4. Dynamic mechanical behaviors

The tan δ curves as a function of temperature for SPU films with different APTES loadings are shown in Fig. 4. As observed, the maximum value of tan δ, shifts from 0.19 for low APTES concentrations (1 wt.%) to values of about 0.14 when large APTES (20 wt.%) concentration was used, as a consequence of more stiff material. In

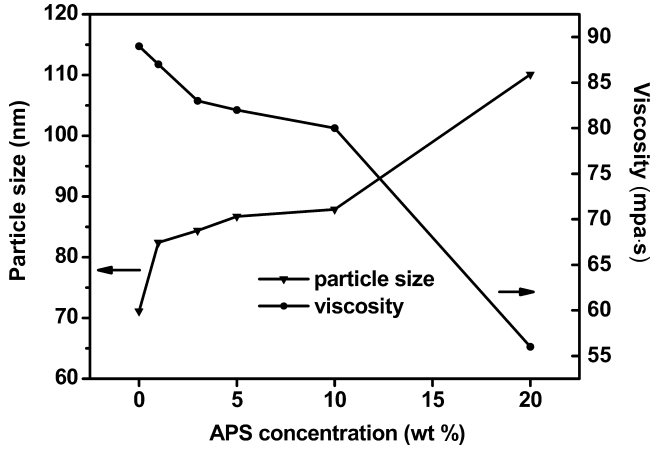

Fig. 2. Effect of APTES content on the SPU dispersions.

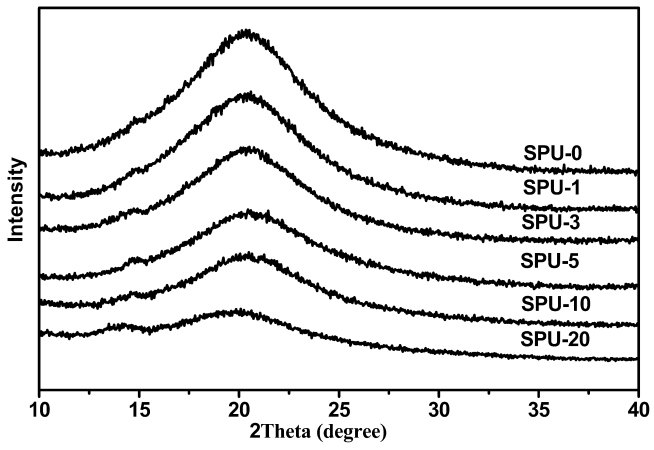

Fig. 3. X-ray diffractograms of SPU.

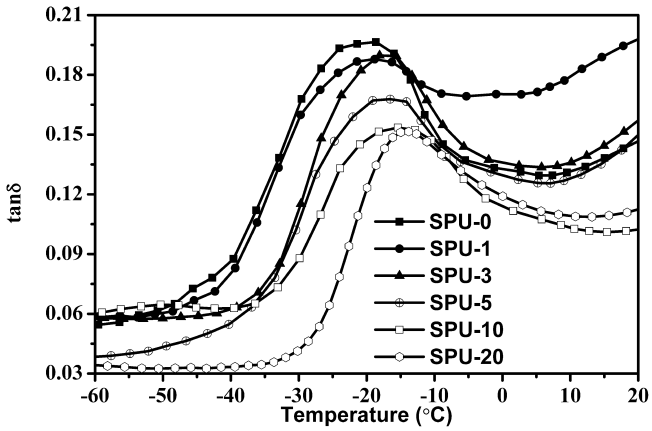

Fig. 4. The loss factor as a function of temperature for SPU.

Table 2
Mechanical properties of the SPU films.

	SPU-0	SPU-1	SPU-3	SPU-5	SPU-10	SPU-20
E (MPa)[a]	8.0	42	33.6	54.6	106.8	451
σ (MPa)	6.5	10.2	13.5	12.6	18.5	19
ε (%)	430	240	210	180	143	96
Toughness (MPa)	18.6	18.5	19.2	15.8	22.1	17.6
Pencil hardness	HB	HB	1H	1H	2H	3H

[a] Young's modulus, σ = tensile strength; ε = elongation at break.

addition, the glass transition temperature (T_g) which is assigned to the behavior of the soft polycarbonate diol segment, significantly raised with an increasement of the APTES content. This can be explained in that more APTES incorporated into polyurethane chains retarded the motion of soft segment and induced long relaxation times to follow.

3.5. Mechanical properties

Table 2 summarizes the Young's modulus, tensile strength, elongation at break, and toughness of the SPU films with different content of APTES, and typical tensile stress–strain behaviors are shown in Fig. 5. The SPU-0 shows a Young's modulus of 8.0 MPa, a tensile strength of 6.5 MPa, and an elongation at break of 430%.When the content of APTES increases, the Young's modulus and ultimate tensile strength increase, but its elongation at break decreases. We note that SPU-0 exhibits a strain recovery of 99%

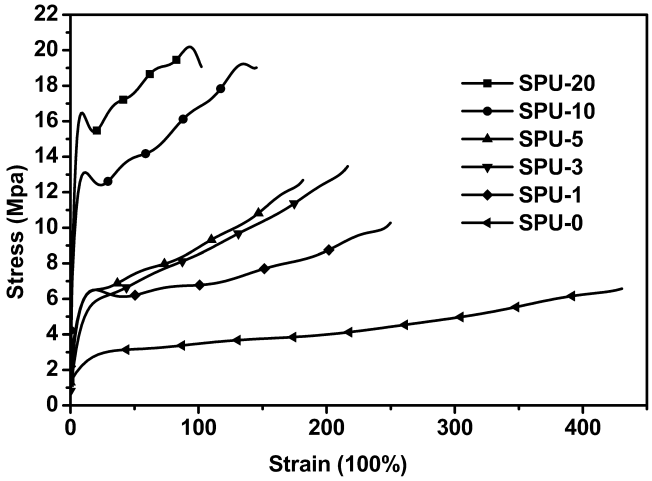

Fig. 5. Stress–strain curves for SPU.

(determined as described elsewhere) and this behavior is similar to the behavior of an elastomeric polymer. However, the films of SPU-1, SPU-3 and SPU-5 exhibit behavior that are typical of ductile plastic with a clear yield point and show a modulus and a tensile strength that are higher than those of SPU-0.The higher content of APTES results in a relatively hard plastic SPU-10 and SPU-20, which exhibit yielding behavior, followed by the strain softening and strain hardening behavior are observed before the specimen breaks. Besides the tensile strength and the Young's modulus, the toughness which indicates the amount of energy per volume that a material can absorb before rupturing, is also calculated from Fig. 5 by integrating the area under the stress-strain curves [11]. The toughness of the resulting SPU films is illustrated in Table 2. It is shown that the adding of APTES does not affect the toughness significantly. This observation is interesting as it indicates the introduction of APTES does not change the toughness of this polymer system. The pencil hardness measurements which test the ability of scratch resistance of a surface posed by pencils of varied hardness were also determined. The values of pencil hardness are shown in Table 2. It is evident that as the content of APTES increased, the ability of scratch resistance enhanced, especially when the content of APTES increase to 20%, the 3H pencil could not mar the surface. It is believed that hardness corresponds to the resistance of a material to localized plastic deformation which includes the breakage of bonds with original atom neighbors and reformation of new bonds as large numbers of atoms or molecules move relative to one another [28]. The incorporation of Si—O—Si chains into the polyurethane backbone increasing the cross-linking density and the rigidity of the films which in turn lead to more resistant of the films to localized plastic deformation as it becomes more difficult for bonds to break and reform new bonds.

3.6. SEM analysis of surface morphologies

The surface morphologies were studied by SEM and shown in Fig. 6. The films SPU-0 and SPU-1 display a rough surface with some wave-like belts distributing in the whole region homogenously. As the APTES incorporation increasing, the surface of the films exhibits less rough morphologies, evidenced by the SPU-3 and SPU-5 microphotographs in Fig. 6. For the SPU-10 and SPU-20 films, smooth surface are evident which are significantly different from the films containing low incorporation of APTES. It is known that as to segmented PU block copolymers, combination of their chemical composition, block lengths, and thermodynamic miscibility between hard and soft segments plays an important role on the formation of the phase-separated microstructure. In our case, the hard segments are composed of urethane and urea groups, and soft segments are composed of polyester carbonyls and Si—O—Si chains. Form the obtain results of FTIR and XRD, we found that the disordered hydrogen bonds increases with increasing APTES give rise to a higher degree of hard/soft-segment mixing. Herein, we consider the domains of soft segments and the intermediate phase as the matrix. The domains of hard segments are more dispersed and encapsulated in the matrix [29]. The compatibility between hard and soft segments results in surfaces ranging from strongly phase separated to nearly homogeneous.

3.7. Swelling of SPU films in water and toluene

It is well known that water and toluene resistance are important properties of the water-based polymer systems. Water and toluene swelling of the SPU films were tested and listed in Table 1. The modified WPU samples exhibited much lower swelling ratios than that of pure PU because the siloxane networks hind the solvent (water or toluene) molecule from getting into the bulk. Moreover,

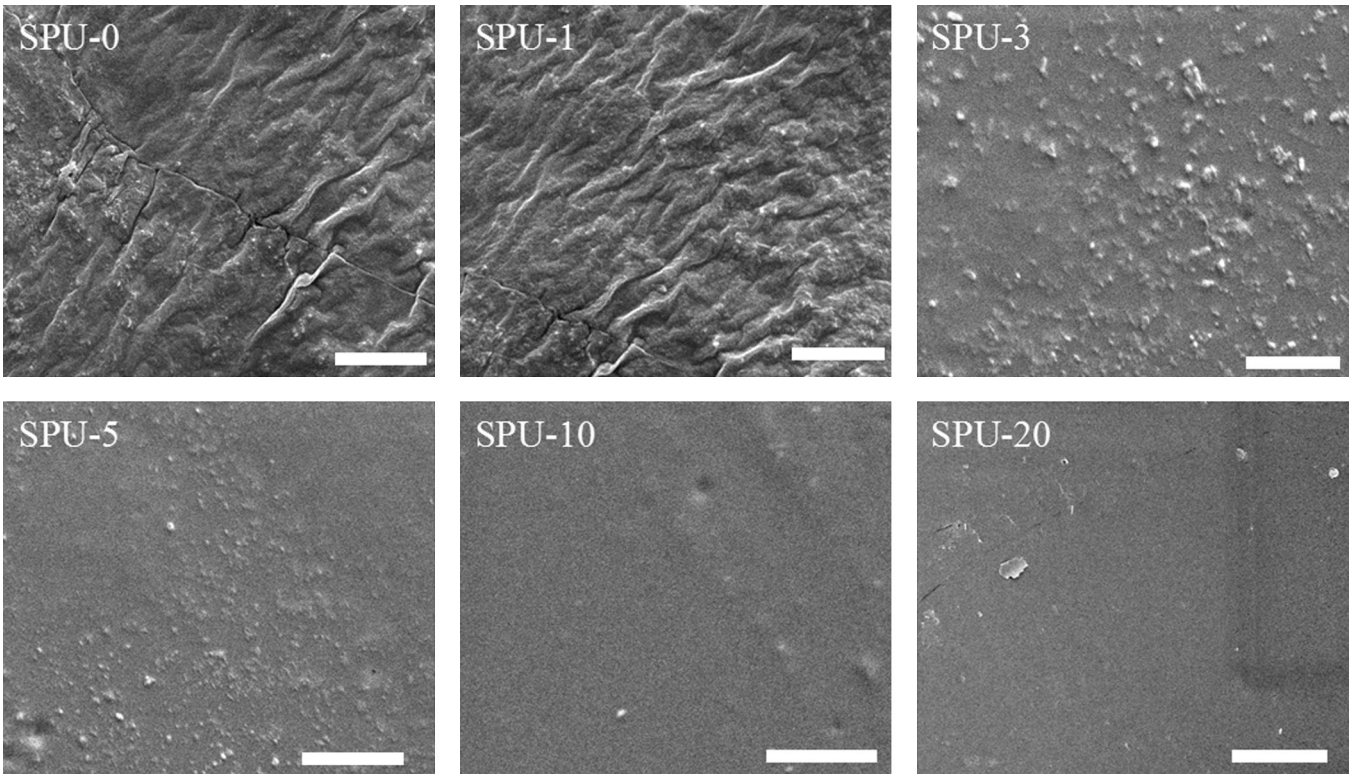

Fig. 6. SEM microphotographs of the surface of SPUs films (scale bar = 10 μm).

the siloxane group was hydrophobic and hence improved the water swelling remarkably.

3.8. Thermal properties of SPU films

The TGA curves of the SPU films are shown in Fig. 7 and temperatures at which 10% (T_{10}) and 50% (T_{50}) weight loss occurred are summarized in Table 1. The onset decomposition temperatures of the SPU are somewhat different, but this difference is not significant. However, the temperatures of T_{10} and T_{50} shift from 290 to 302 °C and from 330 to 356 °C, when the content of the SPU increased from 0 wt% to 20 wt%. This can be explained by the siloxane (Si—O—Si) network incorporated in the urethane segment and restrained the volatilization of the chain. Also, there is an increase in char formation due to the presence of the silica formed in the alkoxysilane groups condensation process.

3.9. The transparency of the coatings

The transmission spectra of SPU coatings in the wavelength range of visible light (400–780 nm) as a function of APTES content are given in Fig. 8. Compared with the pure WPU coating, the transmittance of SPU coatings in visible light began to decline slightly as APS load increasing. In the case of SPU-20 coating, the declination of transmission was pronounced, however it still presented high transparence. There are two factors influence the transparence of the coatings. On the one hand, the incorporation of APTES into the PU chain favoring the phase mixing would lead to more amorphous of PU phase and then more transparent of the coatings. On the other hand, the silica nanopaticles formed due to the alkoxysilane groups undergo hydrolysis and condensation reactions during the

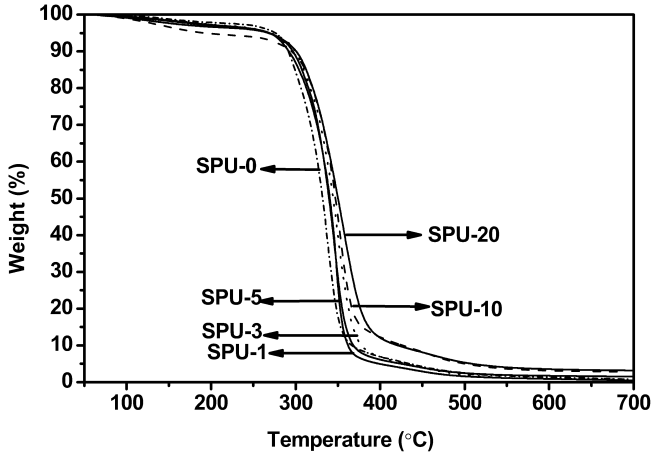

Fig. 7. TGA of the SPU films.

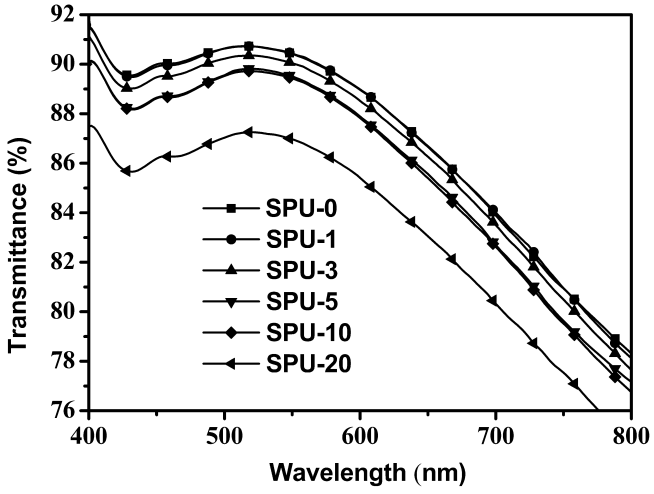

Fig. 8. Transmittance spectra in the visible range.

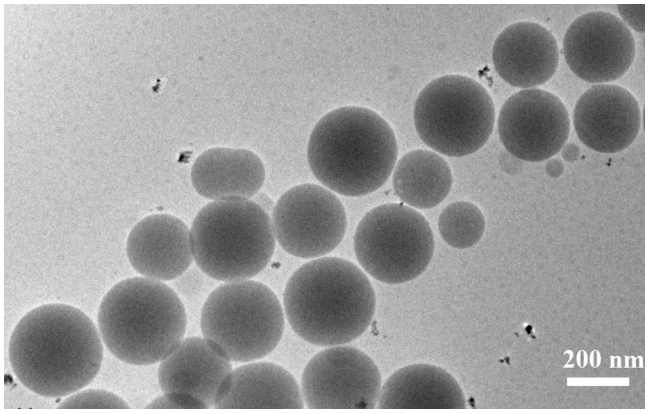

Fig. 9. TEM photograph of SPU-20 dispersion.

phase inversion process of APTES terminated polyurethane have negative effect on the transparence [30]. In order confirm the silica nanopaticles formation, TEM was carried out. Fig. 9 shows image of SPU-20 dispersion. It can be seen that spherical nano silica present with dimater larger than 100 nm. The loss of transparency owing to light scattering can be explained by Eq. (1) below.

$$T = \frac{I}{I_0} = \exp\left(-\left[\frac{3V_p \times r^3}{4\lambda^4}\left(\frac{n_p}{n_m} - 1\right)\right]\right) \quad (1)$$

where T is the transmittance of incident light, I and I_0 are the transmitted and incident light intensity, V_p is the volume fraction of inorganic particles, r is the radius of spherical particles, χ is the optical path length, λ is the wavelength of incident light, and n_p and n_m are the refractive index of nanoparticles and matrix [31]. Eq. (1) shows that the different refractive indexes of the silica nanopaticle ($n \approx 1.45$) and PU polymer matrix ($n \approx 1.58$) as well as relatively large size of the silica nanopaticles are responsible for reduction in the transmittance of nanocomposites in the visible range [32]. Thus, it can be inferred that the formation of silica nanopaticles was the dominating factor influencing the transparency of the coatings, especially for high APTES was introduced.

4. Conclusions

In this study, waterborne polyurethane dispersions modified with different concentrations of APTES were successfully obtained through the acetone process. The incorporation of the alkoxysilane groups into the polyurethane backbone was confirmed by means of FTIR analysis. Further analysis of the FTIR spectra revealed that stronger phase mixing on the interface between hard and soft segments as a result of the increasement of APTES content. The stronger phase mixing disturbed the ordered arrangement of polymer chains that were demonstrated by X-ray diffraction. The effect of the APTES concentration on the particle size and morphology were also investigated and the results showed that the average particle size and viscosity changed slightly when the loading of APTES lower than 10%. However, when it increased to 20%, those changes were pronounced. The mechanical and thermal properties of alkoxysilane modified WPU were superior to that of pure WPU. Moreover, the films of SPU showed higher water and toluene resistance and excellent transparence, thus APTES modified WPU can be used as wood varnish, leather polish, glass coating, decorative and protective coatings.

Acknowledgments

The authors are grateful to the support of National Natural Science Foundation of China (No. 51103160).

References

[1] Z.S. Petrovic, J. Ferguson, Prog. Polym. Sci. 16 (1991) 695–836.
[2] M.A. Osman, V. Mittal, M. Morbidelli, U.W. Suter, Macromolecules 36 (2003) 9851–9858.
[3] O. Ihata, Y. Kayaki, T. Ikariya, Angew. Chem. Int. Ed. 43 (2004) 717–719.
[4] M. You, X. Zhang, J. Wang, X. Wang, J. Mater. Sci. 44 (2009) 3141–3147.
[5] Y.J. Li, T. Tomita, K. Tanda, T. Nakaya, Chem. Mater. 10 (1998) 1596–1603.
[6] Q. Zhang, J. Hu, S. Gong, J. Appl. Polym. Sci. 122 (2011) 3064–3070.
[7] A.B. Jozwiak, C.M. Kielty, R.A. Black, J. Mater. Chem. 18 (2008) 2240–2248.
[8] H. Tanaka, Y. Suzuki, F. Yoshino, Colloids Surf. A 153 (1999) 597–601.
[9] Y.S. Lu, R.C. Larock, Biomacromolecules 8 (2007) 3108–3114.
[10] B.U. Ahn, S.K. Lee, J.H. Park, B.K. Kim, Prog. Org. Coat. 62 (2008) 258–264.
[11] Y.S. Lu, R.C. Larock, Biomacromolecules 9 (2008) 3332–3340.
[12] J.W. Gooch, H. Dong, F.J. Schork, J. Appl. Polym. Sci. 76 (2000) 105–114.
[13] H. Sardon, L. Irusta, M.J. Fernandez-Berridi, M. Lansalot, E. Bourgeat-Lami, Polymer 51 (2010) 5051–5057.
[14] X. Wang, Y.A. Hu, L. Song, W.Y. Xing, H.D. Lu, P. Lv, G.X. Jie, Surf. Coat. Technol. 205 (2010) 1864–1869.
[15] B.K. Kim, J.W. Seo, H.M. Jeong, Eur. Polym. J. 39 (2003) 85–91.
[16] H.Y. Choi, C.Y. Bae, B.K. Kim, Prog. Org. Coat. 68 (2010) 356–362.
[17] X.D. Cao, H. Dong, C.M. Li, Biomacromolecules 8 (2007) 899–904.
[18] J.-J. Chen, C.-F. Zhu, H.-T. Deng, Z.-N. Qin, Y.-Q. Bai, J. Polym. Res. 16 (2008) 375–380.
[19] A. Lopez, E. Degrandi-Contraires, E. Canetta, C. Creton, J.L. Keddie, J.M. Asua, Langmuir 27 (2011) 3878–3888.
[20] U. Sebenik, M. Krajnc, Colloids. Surf. A 233 (2004) 51–62.
[21] Y. Chujo, T. Saegusa, Adv. Polym. Sci. 100 (1992) 11–29.
[22] Y.C. Shi, Y.S. Wu, Z.Q. Zhu, J. Appl. Polym. Sci. 88 (2003) 470–475.
[23] H. Sardon, L. Irusta, P. Santamaria, M.J. Fernandez-Berridi, J. Polym. Res. 19 (2012).
[24] D.K. Lee, H.B. Tsai, R.S. Tsai, J. Appl. Polym. Sci. 102 (2006) 4419–4424.
[25] A. Kultys, M. Rogulska, S. Pikus, K. Skrzypiec, Eur. Polym. J. 45 (2009) 2629–2643.
[26] Z.W. Ma, Y. Hong, D.M. Nelson, J.E. Pichamuthu, C.E. Leeson, W.R. Wagner, Biomacromolecules 12 (2011) 3265–3274.
[27] J.W. Cho, S.H. Lee, Eur. Polym. J. 40 (2004) 1343–1348.
[28] L.Y.L. Wu, E. Chwa, Z. Chen, X.T. Zeng, Thin Solid Films (516) (2008) 1056–1062.
[29] M.V. Pergal, J.V. Dzunuzovic, R. Poreba, S. Ostojic, A. Radulovic, M. Spirkova, Prog. Org. Coat. 76 (2013) 743–756.
[30] Y. Xia, R.C. Larock, Macromol. Rapid Commun. 32 (2011) 1331–1337.
[31] A. Philosophical Magazine, P. Tao, A. Viswanath, L.S. Schadler, B.C. Benicewicz, R.W. Siegel, ACS Appl. Mater. Interfaces 3 (2011) 3638–3645.
[32] I.H. Malitson, J. Opt. Soc. Am. 55 (1965) 1205–1208.